COATINGS

UDC 621.357.7:669.58:669.788

EFFECT OF REVERSIBILITY OF STRUCTURE AND PROPERTIES IN HYDROGEN CHARGING OF CARBON STEEL AND INFLUENCE OF HYDROGEN ON FORMATION OF ELECTRODEPOSITED ZINC COATINGS

M. M. Krishtal,[1] I. S. Yasnikov,[1] A. A. Eremichev,[1] and A. A. Karavanova[1]

Translated from *Metallovedenie i Termicheskaya Obrabotka Metallov*, No. 10, pp. 36 – 42, October, 2007.

Specimens of steel 70 are studied before and after alkaline galvanizing and after galvanizing and partial dehydrogenizing. The content of hydrogen and its distribution between the coating and the substrate are estimated. The structures of the substrate metal and of the coating are studied before and after dehydrogenization. Mechanical tests at various rates of deformation of specimens of steel 70 in different initial states are performed. The tests are followed by an analysis of fracture surfaces. The effect of hydrogen on the fracture behavior is evaluated at different rates of deformation of specimens. The effect of reversibility of the structure and properties in "hydrogen charging – dehydrogenization" of the steel is determined and the mechanism of formation of a layered structure of zinc coatings is described.

INTRODUCTION

Hydrogen enters the metal when it is melted and cast, in gas discharge processes, in welding, and in many chemical and electrochemical processes. Hydrogen charging of metals and alloys is accompanied by various structural changes determined metallographically [1 – 5]. Hydrogen can be one of the main causes of the appearance of cavities, blisters, cracks, and flakes in the metal [3, 6]. The appearance of hydrogen depends strongly on the nature of the metal, its purity, alloying elements, stress distribution, flaws, and other factors [7 – 9]. Hydrogen can be present in the metal in different states, i.e., in dissolved condition (atomic hydrogen), in molecular form, and in various bound states [2, 6, 10, 11]. This explains the contradictory data on the dependence of mechanical properties of metals and alloys on the total content of hydrogen in them.

In the process of long-term operation of parts hydrogen can cause noticeable embrittlement of metals and alloys (hydrogen embrittlement) [3, 6, 10]. The specificity of the interaction between hydrogen and metals in plastic deformation manifests itself in lowering of the ductility and elevation of the strength upon decrease in the deformation rate [3, 6]. The lower the deformation rate the more brittle the loaded material becomes, which is an anomaly in itself and hinders the diagnostics of hydrogen brittleness. For example, hydrogen embrittlement can be indeterminable for deformation at a rate of $10^{-4} – 10^{-3}$ sec^{-1} but can lead to failure of the part after long-term operation. A reverse effect is quite possible, i.e., hydrogen can exert a plasticizing action at elevated deformation rates. Today this is used as an operation in pressure treatment of metals (especially of titanium alloys) [3, 6, 11, 12].

Hypotheses explaining these phenomena differ and allow for the interaction of dissolved hydrogen with mobile and immobile crystal structure defects, formation of hydrogen molecules in various sinks (including grain boundaries), and chemical interactions [2, 3, 6, 10, 11, 13].

Hydrogen charging of steel parts is the strongest in electrochemical processes, primarily in zinc and cadmium plating [4, 13 – 15]. Hydrogen charging of carbon steels is accompanied by interaction between hydrogen and carbon, which yields hydrocarbon compounds and can cause irreversible changes in the structure [2, 6, 11]. In critical parts, including springs, hydrogen is often removed from the steel after galvanizing using the operation of dehydrogenizing (heating and holding in the furnace at a temperature of about 200°C for 1 – 3 h), which stimulates, in its turn, changes in the structure and properties of the steel substrate and of the

---

[1] Tolyatti State University, Tolyatti, Russia.

0026-0673/07/0910-0490 © 2007 Springer Science + Business Media, Inc.

coating [15, 16]. After dehydrogenization the roughness of the coating may increase due to the emission of hydrogen. This can degrade the continuity of the coating and the later can lose its protective properties. Dehydrogenization is fraught with fracture of the steel part with phenomena typical for hydrogen embrittlement (intergrain fracture), which indicates that the decrease in the hydrogen content due to the dehydrogenization was insufficient for proper operation.

It is clear that, after galvanizing, hydrogen is present in the steel substrate and in the zinc coating in different states and concentrations, and that the kinetics of the dehydrogenization includes the outcome of hydrogen not only from the steel through the coating but also from the coating itself. The dehydrogenization is affected noticeably by the structures of the steel substrate and of the zinc coating.

Nevertheless, the mechanisms and the kinetics of the dehydrogenization process after galvanizing have not been studied exhaustively. The nature of hydrogen embrittlement of steels, including carbon ones, is also not always clear. No accurate recommendations have been developed on the duration and temperature of dehydrogenizing after galvanizing in domestic and foreign practices, which would allow for the thickness of the steel part, its purpose, and the content of carbon and impurities in the steel. This is responsible for frequent failure of galvanized steel articles (especially of springs) in operation and for their corrosion caused by the initial deterioration of the continuity of the coating as a result of dehydrogenization.

The aim of the present work consisted in determining the regular features of the influence of hydrogen on the structure and properties of galvanized carbon steel (we chose grade 70 for the study) and on the zinc coating after galvanizing and subsequent dehydrogenizing.

METHODS OF STUDY

Flat specimens of steel 70 (the sheet thickness was 1.6 mm) were studied in different states, i.e., the initial state before galvanizing (after quenching and tempering), after alkaline galvanizing (30 min), and after alkaline galvanizing and heat treatment (a hold in the furnace in air at 160°C for 1 h two hours after the galvanizing).

The hydrogen content was determined using an ANVAC gas analyzer in specimens before galvanizing, after galvanizing without dehydrogenizing, and after dehydrogenizing. In order to estimate the kind of the distribution of hydrogen over the thickness of the specimens we additionally determined the hydrogen content in galvanized specimens before and after dehydrogenizing with mechanically removed coating (up to 10 μm of the coating were removed from the plane surfaces).

Mechanical tests in the mode of three-point bending were performed using TiraTEST 2300 (Germany) and H50KT (Tinius Olsen Ltd, Great Britain) devices at various speeds v of displacement of the central bearing (in a range of 0.05 – 120 mm/min). The diameter of the bearing rolls (fixed bearings) was 15 mm; the diameter of the loading roll (the central movable bearing) was 10 mm; the base distances l between the bearings were 66 and 80 mm. We determined the maximum values of the force $P_{\max}$ (N) and of the inflection $\delta_{\max}$ (mm) that corresponded to failure of the specimens. In order to compare the results of the tests on different bases the testing rate was recalculated in terms of the rate of variation of the inflection angle $\varphi = 2v/l$.

The $HV_{0.05}$ microhardness was determined using a Micromet-II device (Germany).

Metallographic studies and analysis of fracture surfaces of specimens after failure were performed with the help of a LEO 1455 VP scanning electron microscope (CARL ZEISS, Germany) with an INCA Energy-300 x-ray power spectrometer.

TABLE 1. Hydrogen Content in Specimens

State of specimens	Amount of hydrogen (average value for three samples), $cm^3/100$ g metal
Without coating	3.0
After galvanizing without dehydrogenizing	12.4
After galvanizing and dehydrogenizing	9.2
After galvanizing and mechanical removal of the coating	6.4
After galvanizing, dehydrogenizing, and mechanical removal of the coating	4.9

RESULTS AND DISCUSSION

The results of the determination of the content of hydrogen are presented in Table 1. Galvanizing increased the hydrogen content from 3.0 to 12.4 cm^3 per 100 g metal of the coated specimen. Further hold at 160°C for 1 h caused partial dehydrogenization, i.e., decreased the hydrogen content to 9.2 $cm^3/100$ g. Comparison of the hydrogen content in galvanized specimens and in specimens with mechanically removal coating shows that the main part of hydrogen after galvanizing is present in the zinc coating. The concentration of hydrogen in the metal of the substrate is virtually twice lower than in the coated specimens both prior to and after the dehydrogenization. By recalculation for the thickness of the coating we can evaluate the concentration of hydrogen in the coating. It amounts to about 400 cm^3 per 100 g coating after galvanizing and to about 200 cm^3 per 100 g coating after dehydrogenizing in a specified mode, i.e., exceeds the concentration in the substrate metal by a factor of 60 and 40, respectively.

Figure 1 presents the structure of the substrate metal before galvanizing, after galvanizing without dehydrogenizing, and after galvanizing followed by dehydrogenizing. The ini-

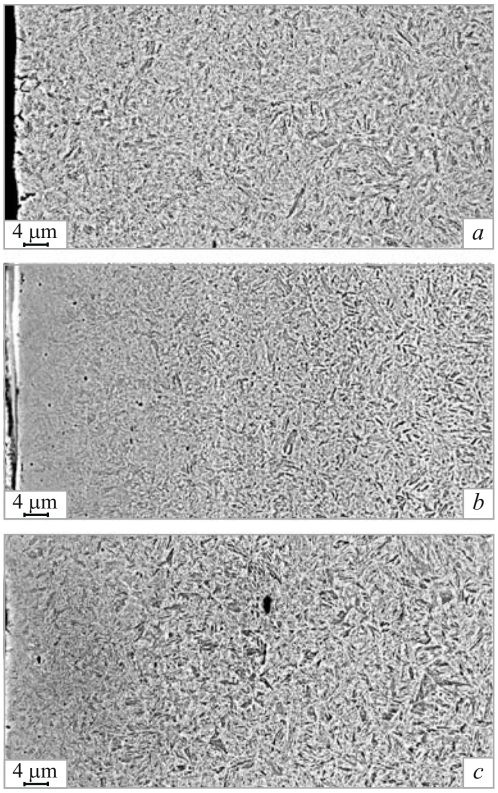

Fig. 1. Structure of steel 70 after quenching and tempering: *a*) before galvanizing; *b*) after galvanizing without dehydrogenizing; *c*) after galvanizing and dehydrogenizing.

tial structure consists of bainite and has no distinctive features over the thickness of the specimens before the operation of galvanizing (Fig. 1*a*). After galvanizing without dehydrogenizing the fineness of the bainite structure increases noticeably at a distance of 15 – 20 μm from the surface; in the core the structure remains virtually unchanged (Fig. 1*b*). As a rule, this effect is identified as partial decarburization due to hydrogen charging [2, 6]. However, x-ray spectrum analysis along a scanning line directed from the surface into the depth of the specimen shows the absence of changes in the carbon concentration over the thickness of the specimens after galvanizing and after galvanizing and dehydrogenizing, which means that no decarburization occurs. Moreover, the structural changes turn out to be reversible; the structure recovers considerably even after incomplete dehydrogenization (Fig. 1*b* and *c*). It can be assumed that such reversible changes in the structure correspond to the decomposition of cementite at preserved local concentration of carbon that passes into other phase components and to subsequent recovery of the cementite upon the removal of hydrogen from the steel at 160°C.

It seems that the structure returns into the initial condition due to formation and decomposition of hydrocarbons. The action of dissolved atomic hydrogen in the decomposition of cementite yields methine (CH), i.e., an unsaturated hydrocarbon, the molecules of which have a quite small size and can reside in crystal lattice defects including subboundary dislocations. The chemical reaction in this case is written as $Fe_3C + H \rightleftarrows CH + 3Fe$. It is obvious that heating for dehydrogenization shifts the chemical equilibrium toward formation of cementite, because in this direction the reaction occurs with decrease in the volume. It should be noted that should the reaction occur with participation of molecular hydrogen instead of atomic one, the situation would have changed for the opposite one, i.e., growth in the temperature would have shifted the equilibrium toward formation of the hydrocarbon [2, 6, 17].

On grain boundaries and in micropores the hydrocarbon is most probably saturated to the marginal state (methane, CH_4). Decomposition of methane at the dehydrogenization temperature is complicated but possible due to the chemisorption on the surfaces of micropores. The decomposition of methane in micropores can be activated by growth in the pressure in the pores upon increase in the temperature for dehydrogenization. The final reaction will have the form

$$Fe_3C + 4H \rightleftarrows CH_4 + 3Fe.$$

The mean values of the microhardness in the core of the specimens after galvanizing before and after dehydrogenizing are virtually similar (with allowance for the confidence intervals) and amount to $394 \pm 9\,HV_{0.05}$ and $400 \pm 7\,HV_{0.05}$, respectively; however they are statistically significantly higher (by about $40\,HV_{0.05}$) than the mean hardness of the core of the specimens before galvanizing, which is equal to $361 \pm 13\,HV_{0.05}$. It is also important that at a distance of up to 10 μm from the surface the microhardness in all states of the specimens is somewhat lower than in the core; in the initial state and after galvanizing the difference is about $60\,HV_{0.05}$, whereas after dehydrogenizing it decreases to $40\,HV_{0.05}$.

These features can indicate hydrogen-induced hardening over the entire thickness of the specimen on one hand and surface softening due to the decomposition of cementite on the other hand. Since the quite substantial decrease in the hydrogen content in the core of the specimens after dehydrogenizing (from 6.4 to 4.9 cm^3 per 100 g metal of the substrate) does not cause decrease in the hardness, we can assume that that the introduction of hydrogen causes hardening irreversible in dehydrogenization, which seems to be connected with local straining.

The morphology of the zinc coating prior to and after dehydrogenizing is presented in Fig. 2. After galvanizing without dehydrogenizing the surface exhibits well manifested boundaries of zinc grains (Fig. 2*a* and *b*). After dehydrogenizing, the whole of the surface of the coating contains closed and opened (burst) round-shape blisters 10 – 30 μm in diameter (Fig. 2*c* and *d*). As compared to the coating not subjected to dehydrogenizing, we can observe thinning of grain boundaries near the burst blisters.

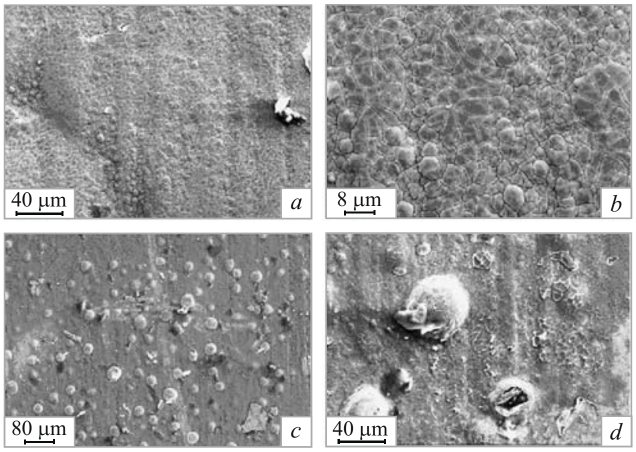

Fig. 2. Zinc coating on steel 70 before dehydrogenizing (*a*, *b*) and after dehydrogenizing (*c*, *d*).

Metallographic analysis of a zinc coating before and after dehydrogenizing showed that it had a layered structure (Fig. 3), which is typical for electrodeposited zinc coatings [18]. The emission of hydrogen over the boundaries of the layers during dehydrogenizing causes formation of lenticular voids (Fig. 4*b*). On the surface these voids are observed as round blisters (Fig. 2*c* and *d*). Such "swelling" of the coating leads to considerable thickening; after dehydrogenizing the thickness of the coating is 7 – 9 μm and individual blister-bearing regions have a thickness attaining 15 μm, whereas after galvanizing the thickness of the coating is 5 – 7 μm. Though the open voids do not propagate through the coating, their formation disturbs the continuity of the passivating layer and lowers substantially the corrosion resistance of the coating.

We studied the layered structure of a zinc coating in greater detail on specimens with a 30-μm-thick coating after long-term natural aging and after subsequent additional heat treatment (240°C for 2 h). Figure 4 shows that the distortions of the shape of the layers repeat the unevenness of the coated surface and damp at a distance from the roughs. The boundaries of the layers represent regions with elevated density of micro- and nanopores (about $10^2 – 10^3$ nm in diameter). The sizes of the pores increase in the course of dehydrogenizing, and the development of the process leads to their merging (compare Fig. 4*a* with 4*b* and *c*). Thus, the initial pores in a zinc coating are sinks for atomic hydrogen; the latter forms molecules increasing the pressure in the pores to a level exceeding first the yield strength and then the strength of the bridges between individual pores, which causes breakage of the bridges.

Formation of a layered structure in zinc coatings can be explained as follows. The electrodeposition occurs with emission of hydrogen. A part of the hydrogen combines into molecules and forms gas blisters kept on the surface of the metal by the force of surface tension. In the process of electrodeposition the blisters continue to grow (by coagula-

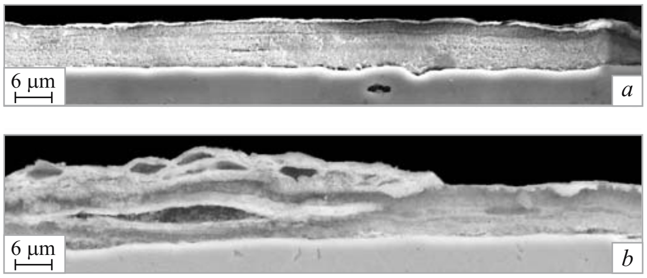

Fig. 3. Zinc coating on a specimen of steel 70 before (*a*) and after (*b*) dehydrogenizing.

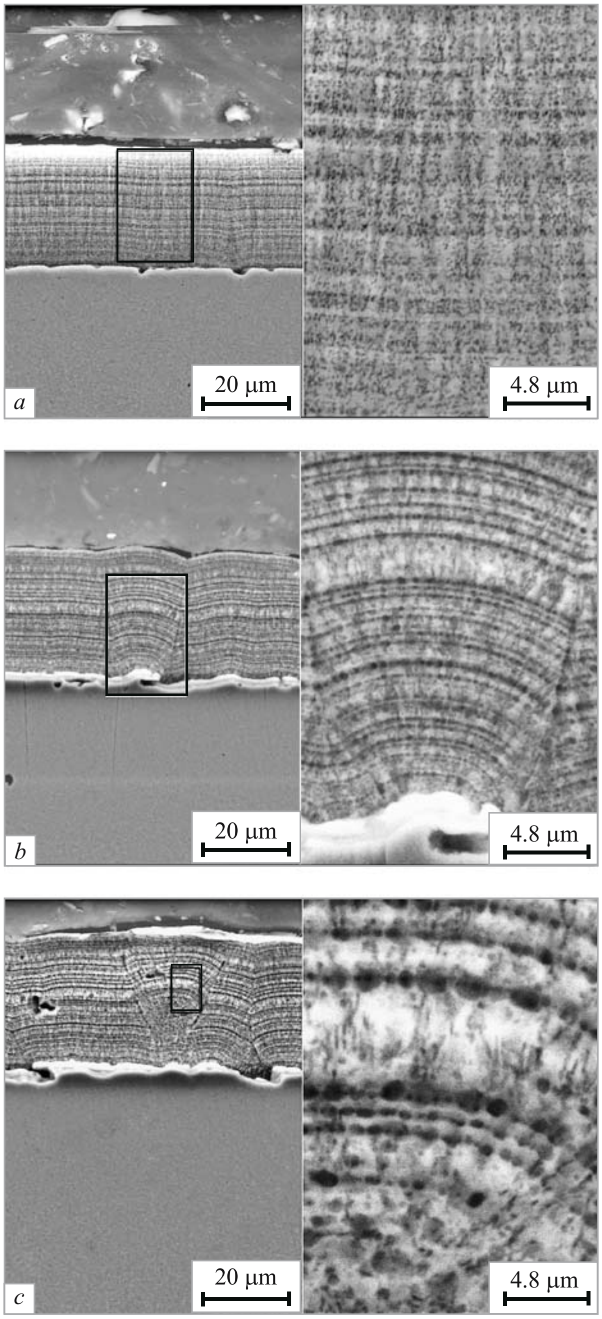

Fig. 4. Zinc coating on a specimen of steel 70 after long-term natural aging (*a*) and after additional heat treatment (240°C, 2 h) (*b*, *c*).

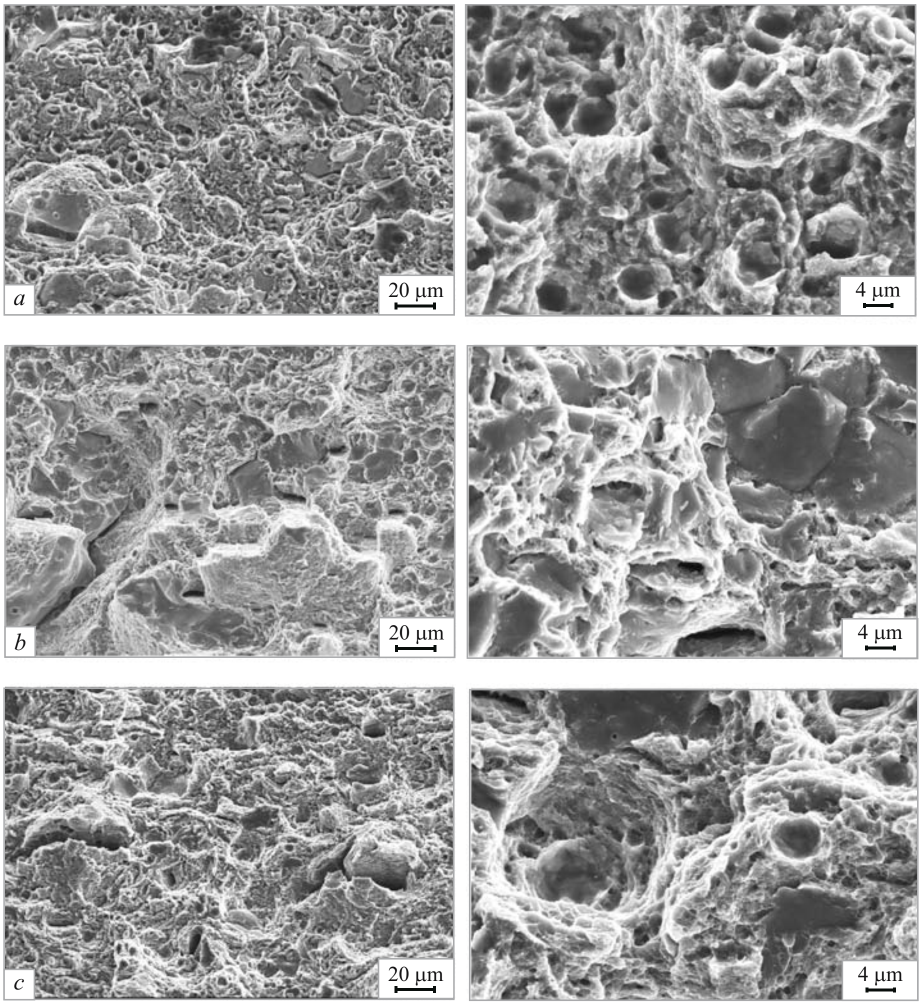

Fig. 5. Fractures of specimens of steel 70 after bending tests at a rate of variation of the deflection angle equal to 6×10^{-4} $\sec^{-1}$: *a*) without coating; *b*) after galvanizing without dehydrogenizing; *c*) after galvanizing and dehydrogenizing.

tion among other ways), attain a specific size, and are detached from the surface of the metal under the action of the lifting force. If the rate of the electrodeposition is high enough, the gas blisters do not have enough time for growing to the required size and are fixed by the deposited metal of the coating. At a constant rate of electrodeposition the number of gas blisters adsorbed on the surface increases, which should accelerate the growth of the coating perpendicularly to the surface, because the coating cannot grow on the blisters themselves. When most blisters of one layer are covered by the coating, the rate of growth of the coating over the normal to the surface decreases. Further appearance of a sufficient number of gas blisters adsorbed on the surface can cause repetition of the process. It seems that such competition in the rates of growth of gas blisters and of the thickness of the coating can result in a self-oscillating regime that leads to formation of a layered distribution of gas (hydrogen-bearing) pores.

The results of mechanical bending tests are presented in Table 2. The nongalvanized specimens exhibit no special features of mechanical properties. In the specimens subjected to galvanizing decrease in the deformation rate causes lower-

TABLE 2. Results of Bending Tests

Rate of variation of deflection angle, $\dot{\varphi}$, $\sec^{-1}$	Determined characteristics*	Condition of specimen		
		without coating	after galvanizing without dehydrogenizing	after galvanizing and dehydrogenizing
2×10^{-5}	$P_{\max}$, N	1030	915	895
(80-mm base)	$\delta_{\max}$, mm	No failure**	10.3	11.9
6×10^{-5}	$P_{\max}$, N	1308	1330	1262
(66-mm base)	$\delta_{\max}$, mm	20.60	10.62	11.04
5×10^{-4}	$P_{\max}$, N	1075	963	935
(80-mm base)	$\delta_{\max}$, mm	No failure**	12.1	17.75
6×10^{-4}	$P_{\max}$, N	1176	1246	1256
(66-mm base)	$\delta_{\max}$, mm	17.75	11.00	10.62
5×10^{-2}	$P_{\max}$, N	1003	926	1050
(80-mm base)	$\delta_{\max}$, mm	No failure**	No failure**	No failure**

* $P_{\max}$ and $\delta_{\max}$ are the maximum values of the force and of the deflection.

** The maximum value of inflection without failure was 17.75 mm.

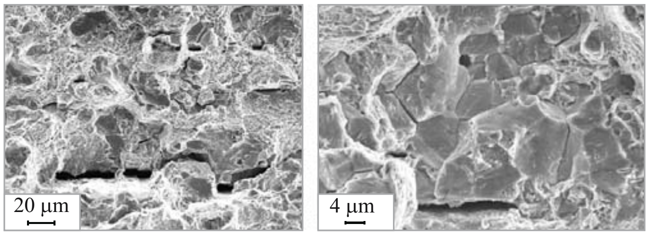

Fig. 6. Fracture of a specimen of steel 70 after galvanizing without dehydrogenizing: bending tests at a rate of variation of the deflection angle equal to 2×10^{-5} sec^{-1}.

ing of the ductility both before and after dehydrogenizing; the tendency is stronger in the specimens not subjected to dehydrogenizing. Such an anomaly is typical for hydrogen brittleness [3, 6, 11].

As an example, we present in Fig. 5 fractures of specimens that have failed in bending tests at a rate of variation of the deflection angle equal to 6×10^{-4} sec^{-1}. Uncoated specimens are characterized by ductile fracture with numerous dimples (Fig. 5*a*). After galvanizing without dehydrogenizing the dimples are virtually absent and the fracture acquires a primarily brittle nature with deterioration over grain boundaries (Fig. 5*b*). In specimens after galvanizing and dehydrogenizing the fracture has an intermediate nature bearing dimples typical for the ductile component and exhibiting intergrain cracking (Fig. 5*c*). Decrease in the deformation rate of hydrogen charged specimens makes the brittle component of the fracture grow, which is obvious from comparison of the fractures obtained for the rates of variation of the deflection angle equal to 6×10^{-4} sec^{-1} (Fig. 5*b*) and 2×10^{-5} sec^{-1} (Fig. 6).

In specimens after galvanizing before and after partial dehydrogenizing cracking in the fractures occurs between individual grains. Another typical feature is the presence of lenticular voids (flakes) that are not intergrain formations but seem to have appeared before the beginning of macroscopic fracture. As an example, such a defect is presented in Fig. 7.

The increase in the proportion of intergrain cracking upon hydrogen charging and reduction of the deformation rate becomes easily explainable if we assume that the grain boundaries are sinks for dislocations moving with atmospheres of atomic hydrogen that gets on grain boundaries, forms molecules, and creates excess pressure. It is obvious that at a lower deformation rate more hydrogen atoms gather in the dislocation atmosphere. At the same time, when the deformation rate is high enough, the hydrogen atmosphere can have no time to form around dislocations.

CONCLUSIONS

1. The effect of reversibility of decomposition of cementite in hydrogen charging of carbon steel has been discovered. The effect manifests itself in segregation of cementite upon subsequent heating that causes dehydrogenization.

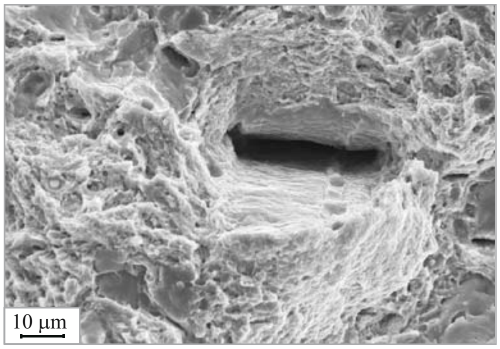

Fig. 7. A flake in a fracture appearing as a result of hydrogen destruction of steel 70 after galvanizing without dehydrogenizing: bending tests at a rate of variation of the deflection angle equal to 6×10^{-4} sec^{-1}.

2. A mechanism has been suggested for explaining the effect of reversibility of decomposition of cementite in hydrogen charging. The decomposition of cementite upon interaction with atomic hydrogen in hydrogen charging of the steel is not accompanied by removal of carbon from the surface of the steel (i.e., decarburization) but causes formation of hydrocarbon compounds that can be preserved in various crystal defects [unsaturated hydrocarbon: methine (CH)] and micropores [saturated hydrocarbon: methane (CH_4)]. Heating of hydrogen-charged steel accompanied by dehydrogenization causes decomposition of the hydrocarbons and formation of cementite; the former two processes are activated by chemisorption on the surfaces of micropores and by growth in the pressure of the gas present in structural traps.

3. The content of hydrogen in an electrodeposited zinc coating before dehydrogenization is 60 times higher than that in the substrate metal (steel 70) and attains 400 cm^3 per 100 g of the coating. A considerable part of hydrogen is present in the coating in molecular form in micro- and nanopores.

4. On the boundaries of layers of electrodeposited zinc coatings the density of the nano- and micropores is elevated and the periodicity of the location of the pores over the thickness is responsible for the layered structure of the zinc coating. Formation of a layered structure is a result of a self-oscillating process that appears due to the competition between the rate of growth of blisters of molecular hydrogen H_2 emitted in the process of electrodeposition of the coating and the rate of growth of the thickness of the coating that fixes hydrogen blisters in the structure.

5. Heating for dehydrogenization causes “swelling” of the coating and the appearance of closed and opened (burst) blisters on its surface. This effect is explainable by the flow of atomic hydrogen into the pores lying primarily on the boundaries of the layers of the coating and by subsequent formation of molecular hydrogen that causes growth and

merging of the micropores under the action of the pressure of molecular hydrogen that opens the pores.

6. Decrease in the deformation rate is accompanied by lowering of the ductility of the hydrogen-charged steel and by appearance of an intergrain fracture component. This is a reflection of the dynamic weakening of grain boundaries upon decrease in the rate of deformation of hydrogen-charged steel and can be explained by formation of atmospheres of dissolved hydrogen on dislocations moving to grain boundaries and by subsequent formation of molecular hydrogen in grain-boundary defects in the deformation process.

The work was performed with financial support from the Russian Foundation for Basic Research (Grant 07-02-96613-r_povolzh'e_a).

REFERENCES

1. O. I. Steklov, N. G. Borodin, V. M. Kushnarenko, and B. V. Perunov, *Tests of Steels and Welded Joints in Hydrogen-Charging Media* [in Russian], Metallurgiya, Moscow (1992).
2. Yu. I. Archakov, *Hydrogen Corrosion of Steel* [in Russian], Metallurgiya, Moscow (1985).
3. B. A. Kolachev, *Hydrogen Brittleness of Metals* [in Russian], Metallurgiya, Moscow (1985).
4. V. V. Kuznetsov, G. V. Khaldeev, and V. I. Kichigin, *Hydrogen Charging of Metals* [in Russian], Mashinostroenie, Moscow (1993).
5. G. M. Pressouyre, *Current Solutions to Hydrogen Problem in Steels*, American Society for Materials International, Materials Park (1982).
6. V. I. Shapovalov, *Effect of Hydrogen on the Structure and Properties of Iron-Carbon Alloys* [in Russian], Metallurgiya, Moscow (1982).
7. Y. Z. Liu, X. T. Zu, C. Li, et al., "Hydrogen embrittlement of a Ti – Al – Zr alloy evaluated by impact test method," *Scr. Mater.*, **52**(9), 821 – 825 (2005).
8. L. Yang and R. B. McLellan, "Effect of palladium on the hydrogen embrittlement of B-doped Ni_3Al," *J. Mater. Res.*, **11**(4), 862 (1997).
9. D. A. Berman, "The effect of baking and stress on the hydrogen content of cadmium plated high strength steels," *Mater. Perform.*, **24**, 36 – 41 (1985).
10. P. V. Geld, R. A. Ryabov, and E. S. Kodes, *Hydrogen and Imperfections in the Structure of Metal* [in Russian], Metallurgiya, Moscow (1979).
11. M. A. Shtremel', *The Strength of Alloys, Part II, Deformation* [in Russian], MISiS, Moscow (1997).
12. V. K. Nosov and B. A. Kolachev, *Hydrogen Plasticizing in Hot Deformation of Titanium Alloys* [in Russian], Metallurgiya, Moscow (1986).
13. A.-M. Brass and J. Chêne, "Hydrogen uptake in 3161 stainless steel: consequences on the tensile properties," *Corrosion Sci.*, **48**, 3222 – 3242 (2006).
14. V. M. Chertov, "Galvanizing: a cause of hydrogen embrittlement of high-strength steel," *Altern. Energ. Ekolog.*, **7**(27), 28 – 31 (2005).
15. Yu. D. Gamburg, *Electrodeposited Coatings: An Application Guide* [in Russian], Tekhnosphera, Moscow (2006).
16. V. P. Maksimchuk and S. P. Polovnikov, *Hydrogen Cracking of High-Strength Steels after Electrochemical Deposition of Coatings* [in Russian], Énergoatomizdat, Moscow (2002).
17. N. K. Meshkov and V. I. Kholodnyi, "Materials and metallurgical processes for power installations on cryogenic components," *Altern. Energ. Ekol.*, **2**(10), 41 – 47 (2004).
18. E. V. Proskurin, V. A. Popovich, and A. T. Moroz, *Galvanizing, A Reference Book* [in Russian], Metallurgiya, Moscow (1988).